Received: 13 April 2021 | Revised: 24 June 2021 | Accepted: 27 July 2021

DOI: 10.1111/ejss.13157

ORIGINAL ARTICLE

European Journal of Soil Science WILEY

Long-term effect of biochar on physical properties of agricultural soils with different textures at pre-industrial charcoal kiln sites in Wallonia (Belgium)

Martin Zanutel[1] | **Sarah Garré**[2] | **Charles L. Bielders**[1]

[1]Earth and Life Institute, UCLouvain, Louvain-la-Neuve, Belgium

[2]Gembloux Agro-Bio Tech, Université de Liège, Gembloux, Belgium

Correspondence
Martin Zanutel, Earth and Life Institute, UCLouvain, Croix du sud 2, bte L7.05.02, B-1348 Louvain-la-Neuve, Belgium.
Email: martin.zanutel@uclouvain.be

Funding information
Fonds De La Recherche Scientifique - FNRS, FRIA; Université Catholique de Louvain; This work is part of a PhD supported by a FRIA grant from the Belgium Fund for Scientific Research (FSR-FNRS).

Abstract

Besides its carbon (C) sequestration potential, biochar is being promoted as an amendment to improve soil quality. Burying biochar in soils is known to affect soil physical quality in the short-term (<5 years), although the intensity of these effects depends on soil texture and biochar concentration especially. However, the long-term effects of biochar remain largely unknown, yet are important to quantify given biochar's persistency in soils. The objective of this study was therefore to assess the long-term effect of biochar on physical properties as a function of biochar concentration for soils with differing textures. For this purpose, soil physical properties were measured in the topsoil of three fields (silt loam, loam and sandy loam textures) in Wallonia (southern Belgium) presenting former kiln sites containing charcoal more than 150 years old. Particle density and bulk density slightly decreased as a function of charcoal-C content but the presence of charcoal in kiln sites did not affect total porosity. The water retention curve measurements revealed that water content was mostly affected in the mesopore range by the century-old charcoal-C content. This effect was strongest for the sandy loam. On the other hand, the presence of century-old charcoal increased the hydraulic conductivity for pF values between 1.5 and 2 for the silt loam, whereas no effect of charcoal was observed for the loamy and sandy loam soils. Results are discussed with respect to biochar characteristics and the various ways in which biochar particles could be distributed within soils. Overall, the present study highlights a limited effect of century-old charcoal on the pore size distribution (at constant porosity) and on the resulting soil physical properties.

Highlights

1. The effect of century-old biochar on physical properties was investigated for 3 different soil textures.
2. Water retention was affected mostly in the mesopore range by biochar.
3. Small effect of biochar on hydraulic conductivity was observed for silt loam soil only.
4. Overall, there was a limited effect of century-old biochar on soil physical properties.

KEYWORDS
biochar, kiln site, soil physical properties, soil texture

1 | INTRODUCTION

Biochar is a solid material obtained from thermochemical conversion of biomass (manure, wood, crop residues, ...) in an oxygen-limited environment and amended to soils (Lehmann & Joseph, 2015; Trupiano et al., 2017). Addition of biochar to soils is often proposed as a way to store carbon and therefore to mitigate climate change (Lehmann et al., 2006). Indeed, due to their intrinsic chemical recalcitrance to biodegradation, the carbon compounds from biochar are not easily degraded (Singh et al., 2012; Solomon et al., 2007). This pyrolyzed carbon can remain stable in soils for hundreds of years, and biochar has therefore been pointed out as a potential carbon sequestration technology (Lehmann, 2007; Singh et al., 2012; Solomon et al., 2007).

Biochar is also being promoted as a soil amendment to improve crop performance, because of the capacity of biochar to change soil biological functioning and improve soil chemical and physical properties, such as pH, cation exchange capacity (CEC), nutrient retention, bulk density, porosity, plant available water capacity and aggregation (Ding et al., 2016). However, the magnitude of biochar's short-term effects on soil quality has been shown to depend on the nature of the biochar (e.g., source of biomass, pyrolysis temperature), on the rate of application and also on soil characteristics (Biederman & Harpole, 2013; Edeh et al., 2020; Jeffery et al., 2011). For instance, in their meta-analysis Razzaghi et al. (2020) reveal that plant available water content increases on average by 45% in coarse-textured soils, by 21% in medium-textured soils and by 14% in fine-textured soils. Although the greatest positive effects of biochar have generally been observed in soils with a coarse or medium texture (Biederman & Harpole, 2013; Jeffery et al., 2011; Omondi et al., 2016), this is not always the case. Indeed, a review by Blanco-Canqui (2017) revealed that the saturated hydraulic conductivity tends to decrease in coarse-textured soils by 7 to 2,270%, is not significantly affected in medium-textured soils and tends to increase in fine-textured soils by 25 to 328% following the addition of biochar.

Although the short-term effects of biochar on soil properties are well-known, mid- to long-term effects (>5 years) are still little documented, as highlighted in the recent meta-analysis of Edeh et al. (2020). The well-known persistency of biochar in soils and the gradual changes of biochar surface characteristics over time when buried in soils justify further investigation of the mid- to long-term effects (Cheng et al., 2006; Lehmann et al., 2005; Singh et al., 2012). Indeed, progressive oxidation overtime (biochar ageing) generates a high density of oxygenated functional groups (dominance of carboxylic groups) at the surface of biochar (Cheng et al., 2006; Lehmann et al., 2005), resulting in an increase in CEC (Chenget al., 2008; Kerré, Willaert, Cornelis, & Smolders, 2017) and a decrease in hydrophobicity (Criscuoli et al., 2014; Knicker, 2011). On the other hand, the depletion of alkaline metal oxides originally present in the ashes of biochar results in an attenuation of the liming effect of biochar with time (Cheng et al., 2006; Hardy et al., 2016; Hardy, Cornelis, Houben, Lambert, & Dufey, 2016). Moreover, biochar pores may also progressively fill with soil material (Lehmann & Joseph, 2009). Such changes could impact the magnitude of the effects of biochar on the soil properties over time.

Besides an increase in CEC, several authors reported higher exchangeable calcium (Ca^{2+}) and magnesium (Mg^{2+}) - but not potassium (K^{+}) - contents in historical charcoal kiln sites compared to adjacent soils in Wallonia, Belgium (Hardy, Cornelis, Houben, Lambert, & Dufey, 2016; Hardy, Cornelis, Houben, Leifeld, et al., 2016; Kerré, Willaert, Cornelis, & Smolders, 2017). These long-term increases in CEC and exchangeable bivalent cation contents may enhance soil aggregation, resulting in a more favourable soil structure and, consequently, in an improvement of soil physical properties (Bronick & Lal, 2005). Existing studies under temperate climate documented a higher porosity (Schneider et al., 2020), a lower bulk density (Faghih et al., 2018; Schneider et al., 2020), a higher plant available water content (Faghih et al., 2018; Kerré, Willaert, Cornelis, & Smolders, 2017) and a higher saturated hydraulic conductivity (Faghih et al., 2018) in historical charcoal kiln sites compared to adjacent soil. However, none of these studies investigated whether the long-term effects depend on soil texture, as has been observed for the short-term effects. Therefore, our main objective was to assess the long-term effect of biochar on the physical properties of soils of differing textures. We used former charcoal kiln sites as natural models to evaluate the long-term effect of hardwood biochar on agricultural soil properties (Hardy, Cornelis, Houben, Leifeld, et al., 2016). Historically, charcoal was produced for iron melting until the early 19th century in Belgium (Hardy & Dufey, 2012). These kiln sites are found across a range of soil types, offering a unique opportunity to study the long-term (>150 years) effects of charcoal on soil properties across different soil textures.

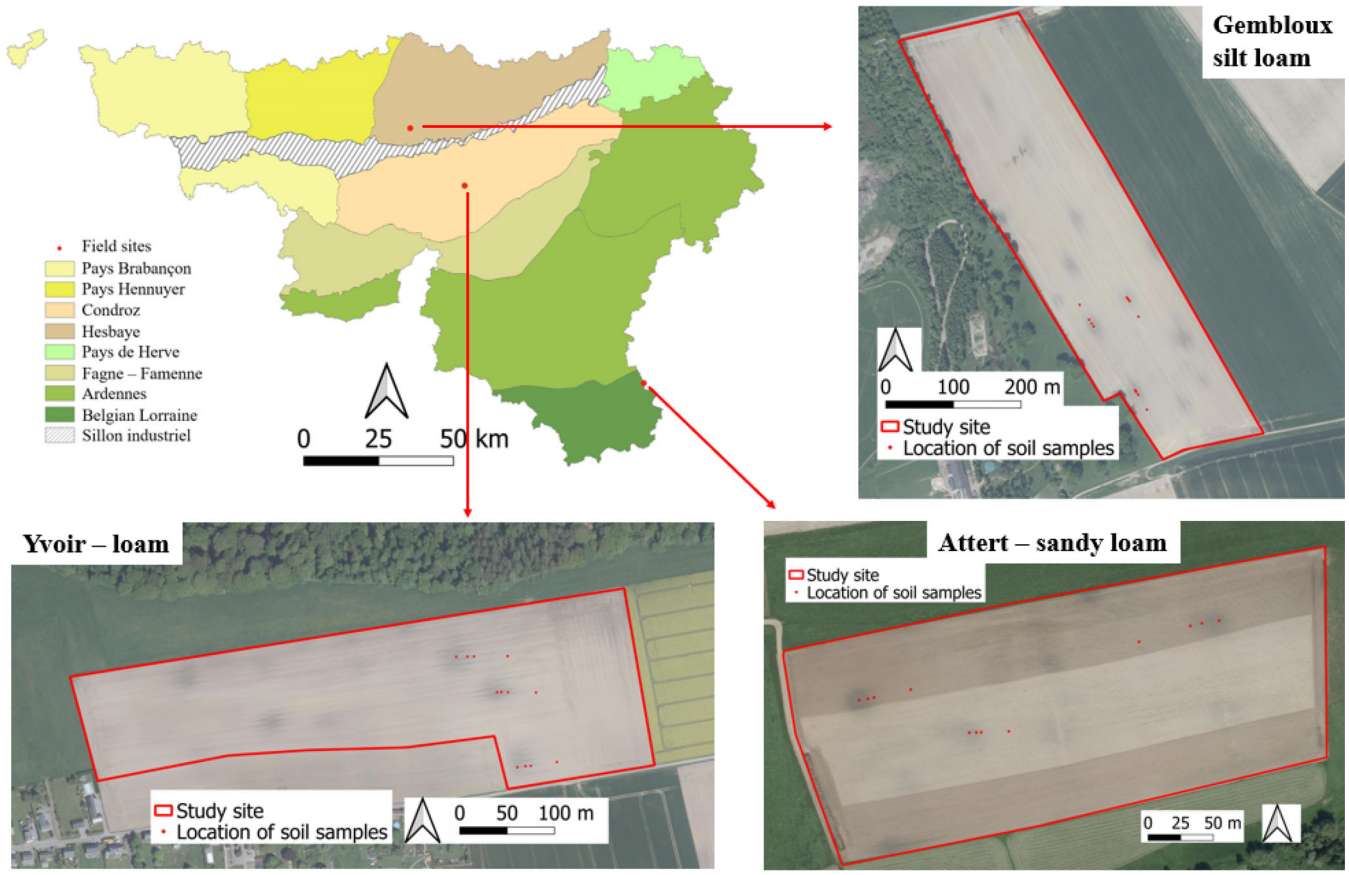

FIGURE 1 Location of the study sites on the Belgian agro-geographic areas map and aerial views showing the soil sampling positions at the silt loam site in Gembloux, the loam site in Yvoir and the sandy loam site in Attert. Kiln sites are visible as darker black spots

TABLE 1 Location and selected characteristics of the study sites: municipalities, latitude (Lat.) and longitude (long.), 30-year (1981–2010) mean annual temperature (T) and precipitation (Prec), field slope, soil texture and gravel content

Municipality	Lat. N (°)	Long. E (°)	T (°C)	Prec (mm)	Slope (%)	Sand (%)	Silt (%)	Clay (%)	Gravel content (%)
Gembloux	4.75	50.52	9.8	834	3	5 ± 1	79 ± 0	16 ± 0	1 ± 0
Yvoir	5.00	50.35	9.4	905	2	35 ± 5	48 ± 5	16 ± 1	13 ± 4
Attert	5.82	49.74	8.8	1,129	4	61 ± 8	26 ± 7	13 ± 1	2 ± 1

2 | MATERIALS AND METHODS

2.1 | Study sites and sampling

Three agricultural fields with charcoal kiln sites from the first half of the 19th century located in Wallonia (southern Belgium) and with distinct soil textures were selected using the digital soil map of Wallonia (Veron et al., 2005) together with aerial images. The sites are located in the municipalities of Gembloux (Loam region), Yvoir (Condroz region) and Attert (Belgian Lorraine; Figure 1). The climate is oceanic temperate (Table 1). The fields in Gembloux, Yvoir and Attert are characterized by a silt loam, a loam and a sandy loam texture, respectively (USDA classification; Table 1).

The chosen fields were forested at the time they were mapped by Ferraris (1770–1778). On the first official topographic survey of the kingdom of Belgium (1865–1880), the sites were no longer covered by forest. Therefore, deforestation occurred between 1770 and 1880, which corresponds to the rise of the steel industry in Belgium, which used vast quantities of charcoal to meet energy demands. The kiln sites are prior to deforestation and most likely from the period 1750–1830, which corresponds to the peak of preindustrial steel manufacturing in

Wallonia (Hardy & Dufey, 2012). Recent aerial images of the selected fields show black spots 10–20 m in diameter corresponding to charcoal kiln relics (Hernandez-Soriano et al., 2016; Kerré, Bravo, Leifeld, Cornelissen, & Smolders, 2016). These black spots are characterized by a decreasing charcoal-C content from the centre outwards. Preindustrial charcoal is assumed here to have the same characteristics for the three sites. Hardy et al. (2017) demonstrated that the charcoal at former kiln sites was dominated by oak (*Quercus robur L.*) and hornbeam (*C. betulus L.*). This century-old charcoal is characterized by a high specific surface area related to its porosity, a high cation exchange capacity and a high carbon content dominated by aromatic-C with a significant fraction of oxygen-rich functional groups such as carboxyl, carbonyl and O-alkyl (Hardy et al., 2017). More information on the chemical properties of century-old charcoal can be found in Hardy et al. (2017) and in Burgeon et al. (2021).

All the three study sites are under conventional soil management, including ploughing, the burying of soil amendments and seedbed preparation. During the growing season, the fields are also sprayed depending on the crop and disease pressure. The fields in Gembloux and Yvoir follow a crop rotation established more than 30 years ago and alternate between chicory, winter wheat, sugar beet, potatoes and winter cover crops (mustard and phacelia) when applicable. In Attert, it has been a monoculture (maize) since approximatively 1970, with winter cover crops.

Soils from the three sites were sampled approximatively 1 month after the last tillage operation. Mustard, winter barley and wheat were sown on 15 September, 5 October and 13 October in Gembloux, Yvoir and Attert, respectively. The preceding spring crops were chicory in Gembloux, sugar beet in Yvoir and maize in Attert. Sampling took place on 25 October, 8 November and 15 November in Gembloux, Yvoir and Attert, respectively. Three charcoal-enriched spots were selected for each site. The topsoil (5–15 cm) was sampled at three positions along the gradients of charcoal concentration, from the centre to the edge of the "black spots", and at one position located more than 20 m from the kiln sites (Figure 1). The latter soil samples served as reference samples. At each position, bulk soil samples and one undisturbed sample (250 cm^3 ring) were taken, leading to a total of 12 bulk and undisturbed samples at each field site. Bulk soil samples were air-dried and sieved (<2 mm) and undisturbed soil samples were stored at 4°C.

2.2 | Soil chemical properties

Soil chemical properties were determined on the bulk samples. Soil pH (ISO 10390) was measured using a glass electrode in a 1:5 (volume fraction) suspension of soil in water (pH-H_2O) or in 1 M potassium chloride solution (pH-KCl). Carbon content was measured by dry combustion (Vario MAX analyser, Elementar). Charcoal-C content was estimated by calculating the difference in carbon content between a given sample and the corresponding reference sample:

$$Charcoal\_C_i = C_i - C_{ref}, \quad (1)$$

with $Charcoal\_C_i$ the charcoal-C content at the position "i" on the gradient of charcoal-C content in a kiln site, C_i the C content at the position "i" on the gradient of charcoal-C content in a kiln site and C_{ref} the C content at a position located more than 20 m from the kiln sites.

Cation exchange capacity in soils was measured using a hexaminecobalt trichloride solution as extractant

TABLE 2 Soil chemical properties (mean ± standard deviation) of the different sites (centre (Ctr) of the kiln sites and reference (Ref.) samples)

		pH-KCl (−)	CEC (cmolc/kg)	K^+	Ca^{2+}	Mg^{2+}
SiL (G)	Ref.	7.4 ± 0.4	11.3 ± 0.2	0.59 ± 0.14	14.6 ± 1.9	0.86 ± 0.02
	Ctr	7.4 ± 0.1	14.0 ± 1.6	0.66 ± 0.06	17.9 ± 1.3	0.96 ± 0.04
	P	0.8703	**0.0007**	0.4172	**0.0009**	**0.0030**
L (Y)	Ref.	6.6 ± 0.2	6.2 ± 0.2	0.36 ± 0.08	9.3 ± 1.0	0.77 ± 0.08
	Ctr	6.8 ± 0.2	11.0 ± 1.1	0.38 ± 0.15	14.7 ± 0.7	0.91 ± 0.04
	P	0.4516	**<0.0001**	0.6860	**<0.0001**	**0.0363**
SaL (A)	Ref.	6.1 ± 0.4	8.6 ± 0.1	0.75 ± 0.15	7.9 ± 0.8	1.36 ± 0.15
	Ctr	6.1 ± 0.2	11.0 ± 0.8	0.71 ± 0.19	10.3 ± 0.8	1.62 ± 0.24
	P	0.8206	**0.0002**	0.8870	**0.0258**	**0.0033**

Note: P corresponds to the *p*-value on the slope of the linear regression between soil chemical properties and the charcoal-C content. Bold values indicate significant relationships ($p < 0.05$). SiL(G) refers to the silt loam soil in Gembloux, L(Y) to the loam soil in Yvoir, SaL(A) to the sandy loam soil in Attert, CEC to the cation exchange capacity and K^+, Ca^{2+}, Mg^{2+} to the exchangeable potassium, calcium and magnesium contents, respectively.

(ISO 23470). Available potassium (K^+), calcium (Ca^{2+}), magnesium (Mg^{2+}) and phosphorus (P) were extracted with a 0.5 M ammonium acetate – 0.02 M ethylenediaminetetraacetic acid (EDTA) solution at pH 4.65 with a 1:5 soil:solution volume ratio (Lakanen & Erviö, 1971) and measured by spectrophotometry.

2.3 | Soil physical properties

Particle density was determined with an air pycnometer (Bielders et al., 1990) on five replicates of 15 g after oven-drying at 105°C (48 h) for each position along the charcoal-C content gradients. After determination of the water retention and hydraulic conductivity curves, bulk density was measured on the undisturbed soil samples by dividing the oven-dry soil mass by the volume of the soil samples (250 cm^3) (Blake & Hartge, 1986). Both particle density and bulk density were used to calculate total porosity of the soil according to the following formula (Danielson & Sutherland, 1986):

$$\text{Porosity} = 1 - \frac{\text{Bulk density}}{\text{Particle density}}. \quad (2)$$

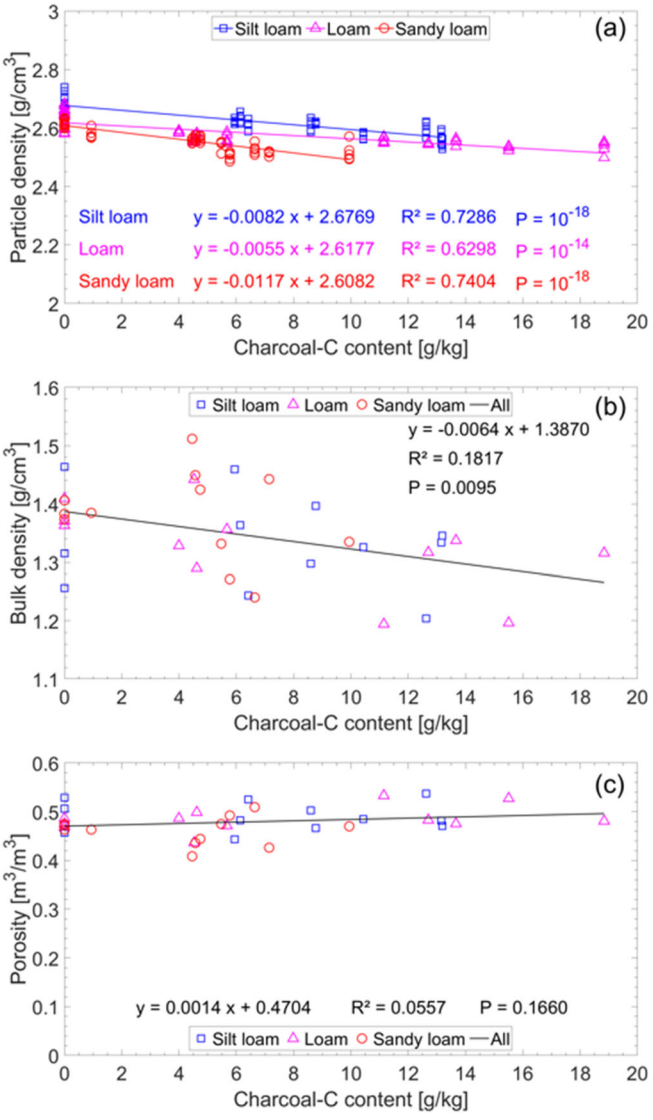

FIGURE 2 Change in particle density (a), bulk density (b) and porosity (c) with charcoal-C content on the silt loam soil (Gembloux), loam soil (Yvoir) and sandy loam soil (Attert). "All" corresponds to the linear regression fitted on the data from the three sites combined and is presented only when the intercept and slope are not significantly different from one site to another. P corresponds to the *p*-value on the slope of the linear regressions

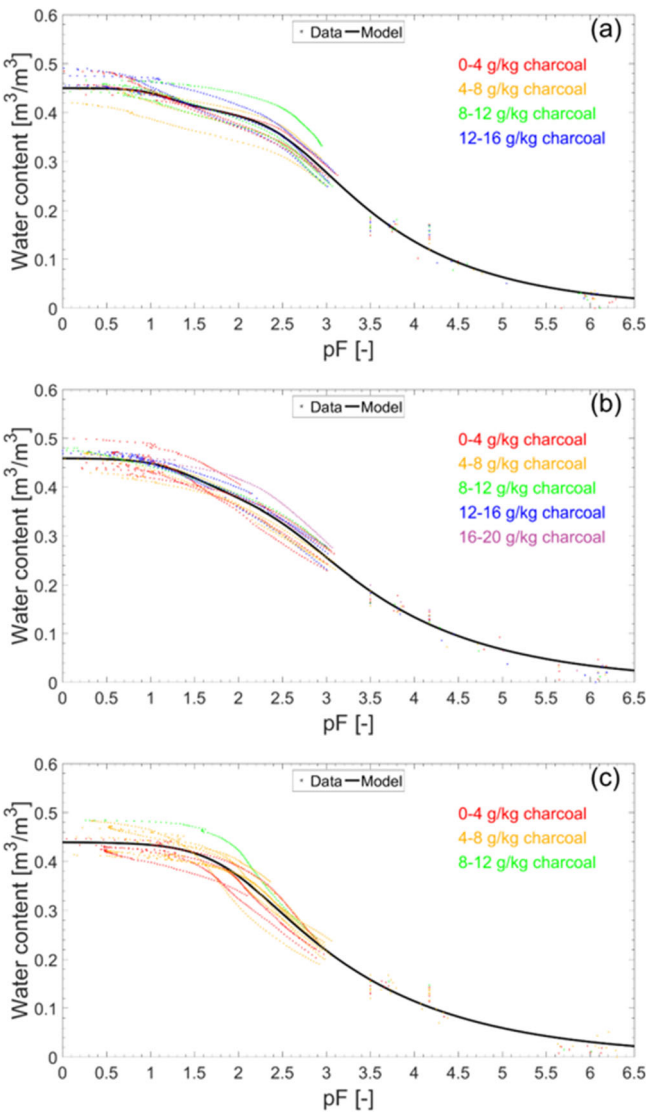

FIGURE 3 Observed and fitted water retention curves for different charcoal-C contents for the silt loam site in Gembloux (a), the loam site in Yvoir (b) and the sandy loam site in Attert (c). Five biochar content classes were defined and a colour attributed to each sample depending on the class to which it belongs. Fitted curves correspond to the Durner model for the silt loam and loam sites, and to the Van Genuchten model for the sandy loam site

TABLE 3 Characteristics of the linear regressions between volumetric water content and charcoal-C content at given matric potentials (h; pF = log(| h |)) at the three study sites

	Gembloux - silt loam			
pF (–)	**Intercept (m^3/m^3)**	**Slope (%v/%m)**	**R^2 (–)**	***p* (–)**
−3.00[a]	0.453 ± 0.010	0.82 ± 1.12	0.051	0.482
0.00[a]	0.451 ± 0.010	0.93 ± 1.21	0.056	0.459
0.50[a]	0.446 ± 0.011	0.90 ± 1.28	0.048	0.496
1.00[a]	0.429 ± 0.011	1.08 ± 1.27	0.068	0.413
1.50[a]	0.403 ± 0.012	1.24 ± 1.44	0.070	0.407
2.00[a]	0.381 ± 0.014	1.05 ± 1.63	0.040	0.533
2.50	0.344 ± 0.014	0.45 ± 1.69	0.007	0.796
3.00	0.276 ± 0.012	−0.06 ± 1.37	0.000	0.965
3.50	0.196 ± 0.007	0.11 ± 0.83	0.002	0.894
4.00	0.132 ± 0.004	0.46 ± 0.51	0.076	0.388
4.20	0.112 ± 0.004	0.57 ± 0.46	0.134	0.243
	Yvoir - loam			
pF (–)	**Intercept (m^3/m^3)**	**Slope (%v/%m)**	**R^2 (–)**	***p* (–)**
−3.00[a]	0.461 ± 0.008	0.73 ± 0.82	0.074	0.393
0.00[a]	0.457 ± 0.009	0.63 ± 0.93	0.044	0.513
0.50[a]	0.453 ± 0.009	0.64 ± 0.89	0.049	0.489
1.00[a]	0.440 ± 0.009	0.80 ± 0.87	0.078	0.380
1.50[a]	0.410 ± 0.008	1.11 ± 0.86	0.144	0.224
2.00[a]	0.367 ± 0.009	1.65 ± 0.93	0.239	0.107
2.50	0.307 ± 0.010	2.03 ± 0.99	0.297	0.067
3.00	0.245 ± 0.008	1.30 ± 0.87	0.185	0.163
3.50	0.189 ± 0.007	0.23 ± 0.68	0.011	0.745
4.00	0.142 ± 0.006	−0.47 ± 0.58	0.060	0.442
4.20	0.126 ± 0.006	−0.65 ± 0.60	0.106	0.302
	Attert - Sandy loam			
pF (–)	**Intercept (m^3/m^3)**	**Slope (%v/%m)**	**R^2 (–)**	***p* (–)**
−3.00[a]	0.426 ± 0.011	4.78 ± 2.05	0.353	**0.042**
0.00[a]	0.421 ± 0.011	5.45 ± 2.04	0.416	**0.024**
0.50[a]	0.419 ± 0.010	5.46 ± 1.98	0.432	**0.020**
1.00[a]	0.414 ± 0.009	5.46 ± 1.79	0.481	**0.012**
1.50[a]	0.394 ± 0.009	5.32 ± 1.79	0.470	**0.014**
2.00[a]	0.349 ± 0.013	4.61 ± 2.51	0.252	0.097
2.50	0.280 ± 0.013	2.75 ± 2.56	0.103	0.309
3.00	0.210 ± 0.010	1.01 ± 1.98	0.026	0.619
3.50	0.155 ± 0.007	0.10 ± 1.45	0.001	0.947
4.00	0.114 ± 0.006	−0.19 ± 1.14	0.003	0.869
4.20	0.101 ± 0.005	−0.20 ± 1.06	0.004	0.855

TABLE 3 (Continued)

	All soils combined			
pF (−)	Intercept (m^3/m^3)	Slope (%v/%m)	R^2 (−)	*p* (−)
−3.00[a]	0.446 ± 0.005	1.66 ± 0.67	0.152	0.019
0.00[a]	0.444 ± 0.006	1.72 ± 0.71	0.146	0.022
0.50[a]	0.441 ± 0.006	1.63 ± 0.70	0.137	0.026
1.00[a]	0.430 ± 0.005	1.55 ± 0.67	0.137	0.026
1.50[a]	0.406 ± 0.005	1.57 ± 0.68	0.134	0.028
2.00[a]	0.365 ± 0.007	2.08 ± 1.02	0.163	0.015
2.50	0.304 ± 0.009	2.60 ± 1.06	0.152	0.019
3.00	0.235 ± 0.008	2.08 ± 1.02	0.109	0.049
3.50	0.173 ± 0.006	1.18 ± 0.73	0.071	0.117
4.00	0.125 ± 0.004	0.53 ± 0.51	0.031	0.308
4.20	0.110 ± 0.004	0.34 ± 0.46	0.016	0.465

Note: "All" corresponds to the linear regression fitted on the data from the three sites combined and P to the *p*-value on the slope of the linear regressions. Bold letters indicate significant relationships ($p < 0.05$).

[a]pF for which the intercept and slope are not significantly different from one site to another.

Both the water retention curve and the hydraulic conductivity curve were determined on undisturbed soil samples. First, soil cores were saturated by capillarity standing in a 0.05 M $CaSO_4$ solution for 1 week. Then, water content and hydraulic conductivity data were collected using a HYPROP device (Pertassek et al., 2015). The HYPROP setup involves pressure head measurements with tensiometers at two depths (1.25 and 3.75 cm). Water contents and fluxes are determined by weighing the sample repeatedly during drying. Hydraulic conductivity data were calculated from measured water fluxes using Darcy's law. The hydraulic conductivity measurement range on the wet side is restricted by limitations of pressure transducers to accurately register very small pressure head differences, and on the dry side by water cavitation in the tensiometers. Improved tensiometers (METER group) were used that resist cavitation up to pressure heads of −30 m thanks to degassing (Schindler et al., 2010). Additional water retention data points were determined using a pressure plate apparatus (−31 m > h > −150 m; Richards & Fireman, 1943) and the WP4C device (h < −150 m; METER Group, 2018). Measured pressure heads, water contents and hydraulic conductivities were subsequently used to derive the water retention and unsaturated hydraulic conductivity functions (Pertassek et al., 2015; Peters & Durner, 2008; Schindler et al., 2010). In this research, two functions were tested for the water retention and hydraulic conductivity curves: the unimodal Mualem-van Genuchten model (van Genuchten, 1980) and the bimodal Durner model (Durner, 1994).

The macropore, mesopore and micropore volumes were calculated based on porosity and defined points on the water retention curve (Rabot et al., 2018). These points depend on the chosen size limits of the pore size classes, for which there are standard limits. Macroporosity was defined as the difference between porosity and water content at field capacity, mesoporosity (also named soil plant available water capacity) as the difference between water contents at field capacity and permanent wilting point, and microporosity as the water content at permanent wilting point. Field capacity corresponds to matric heads generally in the range of −1 to −3.3 m, and permanent wilting point from −50 m and − 300 m (Cassel & Nielsen, 1986; Rabot et al., 2018). In this research, water contents at h = −1 m and at h = −155 m were used as field capacity and permanent wilting point, respectively.

2.4 | Statistical analysis

A linear model between all studied variables (soil properties) and the corresponding charcoal-C content was fitted for each site separately and for all sites combined. The *p*-value on the slope of the linear regressions was used to determine if there was a significant

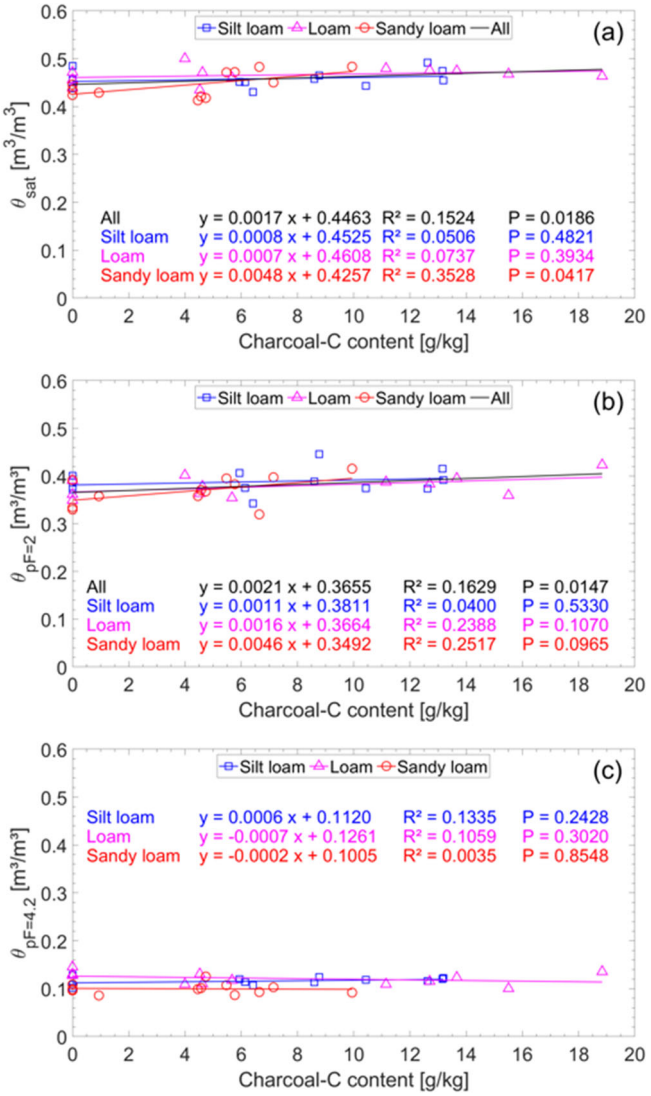

FIGURE 4 Results of the linear regression between water content for different matric heads (at saturation (sat), field capacity (fc; pF = 2) and permanent wilting point (pwp; pF = 4.2)) and charcoal-C content for the silt loam (Gembloux), loam (Yvoir) and sandy loam (Attert) sites. "All" corresponds to the linear regression fitted on the data from the three sites combined and is presented only when the intercept and slope are not significantly different from one site to another. θ corresponds to the water content and P to the *p*-value on the slope of the linear regressions

effect ($p < 0.05$) of century-old charcoal on the dependent variables. The impact of texture on the effect of charcoal was assessed by testing for a difference in slope of the linear models between sites using a paired Student test. Finally, the *p*-value of a paired Student test was used to evaluate if the intercepts of the linear models were significantly different between sites ($p < 0.05$). All the data were analysed using MATLAB (version 2016).

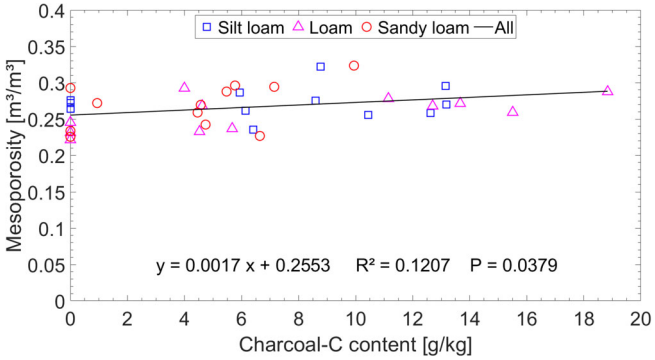

FIGURE 5 Change in mesoporosity with charcoal-C content for the silt loam (Gembloux), loam (Yvoir) and sandy loam (Attert) sites. "All" corresponds to the linear regression fitted to the combined data from the three sites

3 | RESULTS

3.1 | Soil texture, carbon content and chemical properties

The fields in Gembloux, Yvoir and Attert are characterized by a silt loam, loam and sandy loam texture, respectively (USDA classification; Table 1). Clay content was very similar between sites (13–16%; Table 1). On the other hand, the proportion of sand varied widely, from 5% for the silt loam to 61% for the sandy loam soil. Soil texture was not affected by the charcoal-C content (not shown).

Total carbon content (Ctot) in the reference soils was 15.1 ± 0.8 (silt loam), 14.8 ± 0.7 (loam) and 19.8 ± 1.2 g/kg (sandy loam). Ctot concentration at the centre of the kilns ranged from 20.2 to 28.9 g/kg (silt loam), from 26.1 to 34.0 g/kg (loam) and from 25.5 to 30.7 g/kg (sandy loam). After subtracting the Ctot content of the kiln samples from their respective reference samples, the charcoal-C content at the centre of the kilns ranged from 5.9 to 13.2 g C/kg (silt loam), from 11.1 to 18.8 g C/kg (loam) and from 6.6 to 9.9 g C/kg (sandy loam). The sandy loam soil had the highest total carbon content in the reference samples, but the highest charcoal-C content was observed in the loamy soil.

pH-KCl was close to neutral and was not affected by preindustrial charcoal-C content (Table 2). CEC significantly increased with charcoal-C content. Likewise, there were strong significant relationships between exchangeable Ca^{2+} or Mg^{2+} contents and charcoal-C content, unlike exchangeable K^{+} content.

The effects of charcoal on soil chemical properties were not significantly different from one soil type to another, except for exchangeable Mg^{2+} contents (not

shown). The slope of the linear regression between exchangeable Mg^{2+} content and charcoal-C content was significantly higher for the sandy loam compared to the silt loam ($p = 0.0392$) and the loam ($p = 0.0469$), indicating a higher impact of charcoal-C content on Mg^{2+} content for the sandy loam.

3.2 | Particle density - bulk density - porosity

Soil particle density decreased significantly with charcoal-C content for all investigated soil types (Figure 2a).

Soil bulk density values ranged from 1.19 to 1.51 g/cm^3 (Figure 2b) and were very variable. Given the lack of significant differences in slope and intercept between the different soil types, we performed a single regression between charcoal-C content and bulk density for all soils together. Overall, charcoal significantly reduced bulk density (Figure 2b).

Unlike particle density and bulk density, soil porosity was not affected by charcoal-C content and no difference was observed between soil types (Figure 2c). Similar to bulk density, the variability of the measurements was high.

3.3 | Water retention curve

Figure 3 shows the measured water retention curves of all samples and the resulting modelled curve for each soil type. The measured water contents at any given matric head were not significantly affected by charcoal-C content for the silt loam and the loam (Table 3; Figure 4). For the sandy loam, the water content for pF < 2 (pF = log(| h |)) increased significantly with charcoal-C content. At saturation, for example, the water content increases by approximatively 4.8% in volume when the charcoal-C content increases by 1% in mass.

The slopes of the linear regressions between water content at a given matric potential and charcoal-C content were not significantly different between sites. Similarly, no significant difference was found for the intercepts between sites for pF < 2.5. Therefore, linear regressions were also fitted between charcoal-C content and water content at a given pressure potential for the three sites together (Table 3; Figure 4). Overall, water contents for pF ≤3 were significantly affected by charcoal-C contents. The slope of the linear regression between charcoal-C content and water content was largest between pF 2 and pF 3.

In our study, the bimodal Durner model fitted best to the silt loam and the loam curves, whereas the unimodal Van Genuchten model was appropriate for the sandy loam. Model parameters were not significantly impacted by the charcoal-C content for the silt loam and loam. For the sandy loam, only the n parameter ($p = 0.0257$) and the saturated water content ($p = 0.0234$) increased significantly with the charcoal-C content (not shown).

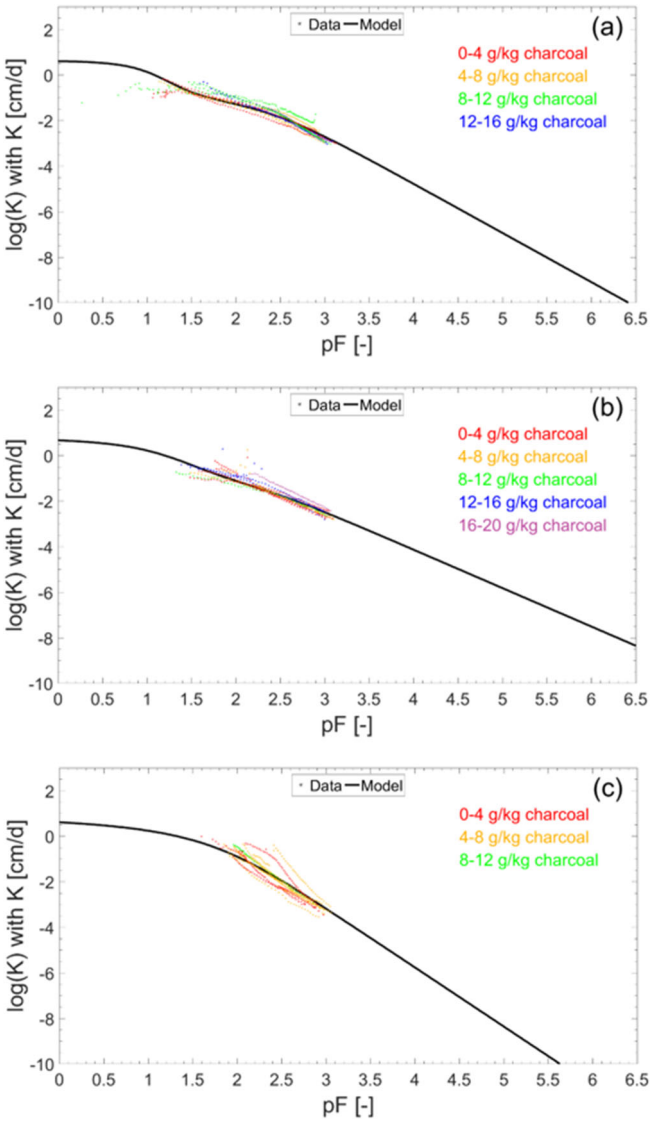

FIGURE 6 Observed and fitted hydraulic conductivity curves for different charcoal-C contents for the silt loam soil in Gembloux (a), the loam soil in Yvoir (b) and the sandy loam soil in Attert (c). Five biochar content classes were defined and a colour attributed to each sample depending on the class to which it belongs. Fitted curves correspond to the Durner model for the silt loam and loam, and to the Mualem-Van Genuchten model for the sandy loam

TABLE 4 Characteristics of the linear regressions between the logarithm of hydraulic conductivity and the charcoal-C content at given matric potentials (h; pF = log(| h |)) at the three study sites

	Gembloux - silt loam			
pF (−)	**Intercept log(cm/d)**	**Slope[a]**	**R^2 (−)**	***p* (−)**
−3.00[b]	1.07 ± 0.51	54.3 ± 59.2	0.077	0.381
0.00[b]	0.82 ± 0.38	33.5 ± 44.0	0.055	0.464
0.50[b]	0.53 ± 0.30	26.5 ± 35.4	0.053	0.471
1.00[b]	−0.02 ± 0.19	24.4 ± 22.5	0.105	0.304
1.50	−0.83 ± 0.09	27.9 ± 10.0	0.439	**0.019**
2.00[b]	−1.39 ± 0.07	26.1 ± 8.6	0.482	**0.012**
2.50[b]	−1.94 ± 0.08	14.2 ± 9.5	0.182	0.167
3.00	−2.70 ± 0.09	−6.2 ± 10.8	0.032	0.576
3.50	−3.63 ± 0.12	−30.2 ± 13.4	0.336	**0.048**
4.00	−4.64 ± 0.15	−53.8 ± 17.2	0.494	**0.011**
4.20	−5.05 ± 0.16	−63.3 ± 19.1	0.525	**0.008**
	Yvoir - loam			
pF (−)	**Intercept log(cm/d)**	**Slope[a]**	**R^2 (−)**	***p* (−)**
−3.00[b]	1.38 ± 0.35	−0.2 ± 35.2	0.000	0.996
0.00[b]	0.96 ± 0.25	1.1 ± 25.6	0.000	0.968
0.50[b]	0.68 ± 0.20	2.5 ± 20.5	0.002	0.904
1.00[b]	0.25 ± 0.17	5.0 ± 16.9	0.009	0.772
1.50	−0.38 ± 0.15	7.3 ± 14.8	0.024	0.632
2.00[b]	−1.05 ± 0.10	9.3 ± 10.4	0.074	0.393
2.50[b]	−1.82 ± 0.05	13.5 ± 5.3	0.394	0.029
3.00	−2.62 ± 0.07	11.9 ± 7.0	0.226	0.119
3.50	−3.47 ± 0.13	5.9 ± 13.5	0.019	0.671
4.00	−4.36 ± 0.22	−0.2 ± 21.9	0.000	0.991
4.20	−4.72 ± 0.25	−2.9 ± 25.7	0.001	0.914
	Attert - Sandy loam			
pF (−)	**Intercept log(cm/d)**	**Slope[a]**	**R^2 (−)**	***p* (−)**
−3.00[b]	1.20 ± 0.24	−25.8 ± 45.6	0.031	0.584
0.00[b]	0.92 ± 0.23	−15.1 ± 44.9	0.011	0.743
0.50[b]	0.76 ± 0.23	−10.6 ± 44.3	0.006	0.815
1.00[b]	0.51 ± 0.22	−5.0 ± 43.3	0.001	0.910
1.50	0.02 ± 0.22	2.0 ± 42.7	0.000	0.964
2.00[b]	−0.77 ± 0.22	8.5 ± 42.4	0.004	0.845
2.50[b]	−1.93 ± 0.19	10.3 ± 36.0	0.008	0.781
3.00	−3.32 ± 0.13	8.7 ± 24.7	0.012	0.733
3.50	−4.79 ± 0.11	7.1 ± 22.1	0.010	0.754
4.00	−6.27 ± 0.18	4.5 ± 34.8	0.002	0.900
4.20	−6.86 ± 0.22	4.1 ± 41.8	0.001	0.924

TABLE 4 (Continued)

	All soils combined			
pF (−)	Intercept log(cm/d)	Slope[a]	R^2 (−)	*p* (−)
−3.00[b]	1.18 ± 0.20	21.1 ± 24.5	0.021	0.395
0.00[b]	0.88 ± 0.15	12.3 ± 18.6	0.013	0.515
0.50[b]	0.66 ± 0.13	7.4 ± 15.6	0.007	0.637
1.00[b]	0.29 ± 0.11	2.3 ± 13.4	0.001	0.867
1.50	−0.31 ± 0.11	−0.8 ± 13.9	0.001	0.957
2.00[b]	−1.00 ± 0.09	4.2 ± 11.6	0.004	0.720
2.50[b]	−1.91 ± 0.06	15.6 ± 7.9	0.102	0.058
3.00	−3.00 ± 0.10	23.3 ± 11.8	0.103	0.056
3.50	−4.18 ± 0.16	26.5 ± 19.8	0.050	0.190
4.00	−5.39 ± 0.23	28.6 ± 28.7	0.029	0.325
4.20	−5.88 ± 0.26	29.3 ± 32.3	0.024	0.371

Note: "All" corresponds to the linear regression fitted on the data from the three sites combined and P to the *p*-value on the slope of the linear regressions. Bold letters indicate significant relationships ($p < 0.05$).

[a] $\frac{\log[\mathrm{cm/d}]\ 10^2}{[\%\mathrm{m.}]}$.

[b] pF for which the intercept and slope are not significantly different from one site to another.

Mesoporosity derived from the water retention curves increased significantly with charcoal-C content overall (Figure 5), unlike macroporosity and microporosity (not shown). Mesoporosity increased on average by 1.7% in volume when charcoal-C content increased by 1% in mass. There was no significant difference between soil types for the macroporosity, mesoporosity and microporosity.

3.4 | Hydraulic conductivity curve

Figure 6 shows the measured hydraulic conductivity curves for all samples and the resulting model for each of the three soil types (bimodal Durner model for silt loam and loam; unimodal van Genuchten model for sandy loam). Saturated hydraulic conductivity and tortuosity parameters were not significantly impacted by the charcoal-C content, except for the tortuosity parameter for the silt loam soil. Nevertheless, it must be noted that the uncertainty on the tortuosity parameter was high.

Modelled values of hydraulic conductivity for all matric potentials were not significantly affected by the presence of historical charcoal in kiln sites for the loam and the sandy loam (Table 4). However, the hydraulic conductivity of the silt loam increased with the charcoal-C content for pF < 3 (significant for pF 1.5 and 2) and decreased for pF higher than 3 (significant for pF ≥3.5).

4 | DISCUSSION

4.1 | Charcoal-C content at kiln sites

The charcoal-C contents were within the range of values reported for cultivated plots with kiln sites in Wallonia (Hardy, Cornelis, Houben, Leifeld, et al., 2016). However, in the present study the charcoal-C content was estimated from the difference in Ctot content of the kiln samples relative to their respective reference samples. Hardy, Cornelis, Houben, Leifeld, et al. (2016) demonstrated for silt loam soils that there was a strong link (r = 0.98) between this way of estimating charcoal-C content and charcoal-C content estimates derived from differential scanning calorimetry. Nevertheless, these authors reported that minor amounts of charcoal (at most 5% of Ctot) can be present in the reference samples due to transport by tillage and other lateral transport processes. Neglecting the presence of charcoal in the reference samples may thus lead to an overestimation (if slope is positive) or underestimation (if slope is negative) of the intercept when plotting the relationship between a given variable and charcoal-C content. However, it does not affect the slope of the regressions. On the other hand, it has also been shown that charcoal has the capacity to enhance the accumulation of uncharred organic carbon content (Burgeon et al., 2021; Hardy, Cornelis, Houben, Leifeld, et al., 2016; Hernandez-Soriano et al., 2016; Kerré et al., 2016). At the centre of kiln sites, Hardy, Cornelis, Houben, Leifeld, et al. (2016), Kerré et al. (2016) and Burgeon et al. (2021) reported on average 1.0 to 1.4 times

more uncharred organic carbon, respectively, than in the reference samples for silt loam soils. A greater amount of uncharred organic carbon content in the kiln sites could possibly be explained by the adsorption of dissolved organic molecules on to the surface of charcoal and physical protection against degradation of organic carbon inside micropores (Burgeon et al., 2021; Hernandez-Soriano et al., 2016; Kerré, Willaert, & Smolders, 2017) or by greater biomass productivity in the presence of charcoal (Jeffery et al., 2011). Accordingly, the results presented here reflect the direct effects of charcoal as well as the effects of any additional uncharred organic carbon that may have accumulated as a result of the presence of such charcoal.

4.2 | Century-old charcoal effect on chemical properties

A lack of effect of charcoal-C on soil pH is consistent with the long-term depletion of alkaline metal oxides present in the ashes of biochar, which have a liming effect in the case of young biochar (Cheng et al., 2006). This lack of effect on soil pH was also reported by Hardy, Cornelis, Houben, Lambert, & Dufey (2016).

In this study, a significant effect of century-old charcoal on soil CEC and exchangeable Ca^{2+} and Mg^{2+} contents was observed, but there was no effect on exchangeable K^{+} content. Hardy, Cornelis, Houben, Leifeld, et al. (2016) and Kerré, Willaert, Cornelis, & Smolders (2017) also reported that kiln site charcoal had no effect on exchangeable K^{+} content, but a significant effect on soil CEC, exchangeable Ca^{2+} and Mg^{2+} contents. The latter studies were limited to silt loam soils. This study thus shows that these effects are also present in loam and sandy loam soils in Wallonia.

4.3 | Century-old charcoal effect on physical properties

The effect of charcoal-C content on soil particle density is rarely measured (Blanco-Canqui, 2017). In the short term, Şeker & Manirakiza (2020) reported a decrease of soil particle density according to biochar content. To our knowledge, such an effect has not been reported hitherto for century-old charcoal in temperate regions. In the present study, the observed decrease in particle density with increasing charcoal-C content can to a large extent be attributed to the lower particle density of biochar compared to soil mineral particles. Abel et al. (2013) and Brewer et al. (2014) reported skeletal particle densities of biochar ranging between 1.5 and 2.0 g/cm^3 for young biochar. Biochar particle densities depend on the type of pyrolyzed biomass and on the production conditions (e.g., temperature; Brewer et al., 2014). Based on the data in Figure 2a, and using a simple mixing model, the skeletal particle density of charcoal was derived from the slope of the linear regression between particle density and charcoal-C content. The resulting charcoal skeletal particle density values range between 0.46 g/cm^3 for the sandy loam and 0.83 g/cm^3 for the loam, with intermediate values for the silt loam (0.64 g/cm^3). These values are significantly lower than those reported by Abel et al. (2013) and Brewer et al. (2014) but of the same order as those reported by, for example, Hardie et al. (2014), 0.51 g/cm^3, or Yi et al. (2020), 0.65 g/cm^3 for hardwood biochar. These low values may in part reflect the contribution of the additional uncharred organic matter that accumulates at kiln sites in the presence of charcoal, as explained above. It may also indicate the presence of occluded porosity in the charcoal particles. Brewer et al. (2014) reported that occluded porosity was mostly observed in biochar produced by slow pyrolysis, which may cause less disruption of cell walls and favour accumulation of tars that may clog pores.

A significant decrease in soil bulk density as a function of charcoal-C content was observed after pooling together the data from all three sites. Similar trends have commonly been reported in the short term (Blanco-Canqui, 2017; Ding et al., 2016; Edeh et al., 2020; Omondi et al., 2016) and long term (Faghih et al., 2018; Schneider et al., 2020). The fact that the bulk density decreases with increasing charcoal-C content can be a direct result of the low particle density of biochar as compared to mineral particles. However, it also indicates that charcoal particles predominantly occupy spaces previously occupied by heavier mineral particles rather than filling voids in between mineral particles. Indeed, if charcoal were to predominantly occupy spaces in between pores formed by mineral particles (e.g., Figure 6 in Edeh et al., 2020), the bulk density should increase with increasing charcoal-C content (i.e., net increase in weight per unit volume). Given that the charcoal at kiln sites has been present in the soil for approximately 150 years and these soils have presumably been cultivated for a large fraction of this time period, an intimate mixing of mineral and charcoal particles is indeed to be expected. Finally, the presence of century-old charcoal is known to affect soil aggregation and could therefore have a structuring effect (Brodowski et al., 2006; Kerré, Willaert, Cornelis, & Smolders, 2017), as will be further discussed below.

Most studies report a positive effect of biochar additions on soil porosity (Blanco-Canqui, 2017), although

the meta-analysis of Omondi et al. (2016) highlighted that this positive effect was only observed for biochar made from crop residues (+11.6%) but not for biochar made from woody material (no significant increase). At kiln sites in Wallonia, oak-derived woody material is the dominant source of charcoal (Hardy et al., 2017), which may in part explain the absence of effect on porosity in the present study. In addition, soil porosity data in the literature must be taken with care because the soil particle density that is needed for the calculation of porosity is not always measured directly, and a constant particle density is therefore assumed. If a constant particle density had been used in the present study, an increase in porosity would also have been reported by virtue of the decrease in bulk density with increasing charcoal-C content (Figure 2b). It appears, however, that at the study sites the decrease in bulk density is being compensated for by the decrease in particle density, leading to a constant porosity, independent of the charcoal-C content. Our results therefore demonstrate the necessity to measure directly soil particle density in future studies in order to properly assess the effects of biochar on soil porosity.

Although the water retention curves were unaffected by the presence of century-old charcoal for the silt loam and loamy soil, higher water contents for pF values lower than 3 in kiln soils compared to adjacent soils were observed for the sandy loam. Kerré, Willaert, Cornelis, & Smolders (2017) similarly observed higher water contents in kiln site soils compared to adjacent soils at most pF values ≤2.8 for a silt loam soil in Belgium. However, the water contents were unaffected by the presence of century-old charcoal for the silt loam and loamy soil. An increase of the plant available water content with the biochar content, as observed in this study, was also reported in the short-term in the meta-analysis of Razzaghi et al. (2020) and in the long term by Kerré, Willaert, Cornelis, & Smolders (2017). The soil hydraulic conductivity curve was unaffected by the charcoal content for the sandy loam and silt loam soils. For the silt loam soil, the hydraulic conductivity increased with the charcoal-C content for pF values of 1.5 and 2, and decreased for pF values higher than 3.5. To our knowledge, the impact of biochar in the long-term on the hydraulic conductivity curve has not been studied. However, Faghih et al. (2018) observed higher saturated hydraulic conductivity in historical charcoal kiln sites compared to adjacent soils in the temperate deciduous forests of Iran. The observed effects on the water retention and hydraulic conductivity curve can be analysed through the effect of century-old charcoal-C content on the soil structure, as developed in the next section.

4.4 | Century-old charcoal effect on soil structure

Although the results indicate a lack of effect of biochar on total soil porosity, this does not imply that biochar has no effect on soil structure because it may still affect pore size distribution and connectivity at constant total porosity. Indeed, the significant overall increases in soil water contents with charcoal-C contents for pF values ≤3 reflect a change in soil structure resulting from the century-old charcoal additions (Table 3; Figure 4). Similarly, the significant changes in hydraulic conductivity observed in the silt loam reflect a change in pore size distribution or connectivity and hence a change in soil structure (Table 4). In general terms, the addition of biochar to soil may modify the internal soil porosity in different ways: (1) through the intrinsic porosity of the biochar particles, some of which may be open to the surrounding soil porosity, some may be occluded and some may be filled with soil material over time (Brewer et al., 2014; Hyväluoma et al., 2018; Lehmann & Joseph, 2009; Yi et al., 2020), (2) by filling voids in between mineral grains, as in coarse-textured soils (Edeh et al., 2020), (3) by occupying space previously occupied by mineral particles or organo-mineral micromass, or (4) by acting as a structuring or a de-structuring element, contributing to soil aggregation (Burgeon et al., 2021; Du et al., 2017) or disaggregation (Pituello et al., 2018). Mechanisms (2) and (3) correspond to a 1:1 vol. replacement of voids or soil micromass, respectively, by an equivalent volume of biochar particles. In (3), the biochar particles are embedded in the soil micromass (see, e.g., Figure 4 in Jien et al., 2015) or behave as single grains (see, e.g., Figure 4 in Jien & Wang, 2013). Mechanism (2) implies a decrease both in total porosity and in the proportion of large pores. Mechanism (3) may lead to an increase, decrease or no change in porosity depending on whether the biochar occupies spaces previously occupied by an (organo-)mineral micromass that had lower (e.g., sand particles), the same or higher (e.g., organo-mineral aggregates) porosity than the biochar. In practice, all four mechanisms could act simultaneously.

The contribution of (1) to the changes in soil water retention and hydraulic conductivity would depend on the intrinsic pore size characteristics of the charcoal. The macro/mesoporosity of biochar being directly derived from the raw biomass (Wildman & Derbyshire, 1991), the intrinsic charcoal porosity must be assessed for oak, the main wood species used for charcoal production during the 19th century in Wallonia (Hardy et al., 2017). Plötze & Niemz (2011) observed a significant macro/mesoporosity of oak with 22% of total pore volume in the range of 2–58 μm. Similar results were reported by Hyväluoma et al. (2018)

with modal pore sizes in the range of 10–20 μm. According to the water retention curves, the effect of charcoal (all soils combined) was observed for pF ≤3, corresponding to a pore diameter > ~3 μm, mostly in the mesopore range (Table 3). Hence, this is compatible with a direct contribution of the intrinsic porosity of charcoal to the observed changes in soil physical properties.

Mechanism (4) would be similar to the aggregating or disaggregating effect of SOM. Century-old charcoal could act as an additional binding agent between organic matter and mineral phases (Burgeon et al., 2021). The formation of bridges between clay and soil organic matter by multivalent cations being one of the several mechanisms of aggregation (Bronick & Lal, 2005), the hypothesis of a structuring effect of charcoal at the study sites could be expected given the outcome of the soil chemical analyses. Indeed, both CEC and exchangeable bivalent cation contents increased significantly with the charcoal-C content (Table 2), which could favour soil aggregation. A higher macroaggregation in kiln sites compared to reference soils has already been reported in the literature (Burgeon et al., 2021). However, biochar could also act as a disaggregating agent, by enhancing the repulsive forces between soil particles with the same charge and monovalent cations (Pituello et al., 2018). This disaggregating process leads to an increase of the microporosity and can take place in clay soil, which is not the case in this study. Nevertheless, because total porosity was unaffected by charcoal-C content and because the soil of the study sites undergoes intense soil management (ploughing, seedbed preparation, ...), it appears that the long-term effect of charcoal on soil structure resulted predominantly from an internal reorganization of particles at the agricultural study sites.

Regarding the contributions of mechanisms 2 and 3, these will be discussed in more detail in the next section.

4.5 | Texture-dependent effect of century-old charcoal

The effect of charcoal on soil physical properties seemed to be most pronounced for the sandy loam soil, although the hydraulic conductivity of the silt loam soil was also affected. This may in part result from differences in the characteristics of the charcoal, as evidenced by the differences in charcoal particle density values, even though oak is expected to be the dominant source of biomass at all sites. Nevertheless, in the short term, the largest effects of charcoal on soil physical properties have also generally been observed in coarse-textured soils as compared to medium- or fine-textured soils (Blanco-Canqui, 2017; Omondi et al., 2016; Razzaghi et al., 2020).

In the sandy loam, bulk density decreased as a result of charcoal addition, but porosity was unaffected. Water content at pF < 2 tended to increase. Although not significant, it can be seen that the slope of the regressions between hydraulic conductivity K and charcoal-C content is negative at small pF values and gradually becomes positive for medium and high pF values (Table 4). These elements may partly indicate the filling of "previous" voids by biochar, leading to lower K near saturation, but at the same time creation of some new porosity in the mesopore range, leading to higher K at high pF values and higher water content at low pF values. Because pore filling would result in a decrease in porosity, which was not observed, the loss in porosity resulting from the filling must have been compensated for by the replacement of (organo-)mineral mass by charcoal of higher porosity.

For the silt loam soil, no effect of charcoal was observed on the porosity and water retention curve but charcoal resulted in an increase in hydraulic conductivity at pF 2 and 2.5. This may indicate some internal restructuring of the soil, with a slight increase in the proportion or connectivity of pores active at pF 2–2.5 but the changes are insufficient to be reflected in the water retention curves. The decrease in hydraulic conductivity at high pF values remains unexplained, however. Nevertheless, the uncertainty on the modelled values of hydraulic conductivity for pF higher than 3.5 was high, so results must be interpreted with care. This uncertainty on the modelled hydraulic conductivity was related to the measurement method as well as the high uncertainty on the tortuosity parameters of the model. Indeed, the method did not allow for the determination of hydraulic conductivity at pF > 3 due to cavitation in the tensiometers.

In the case of the loamy soil, no changes in the water retention curve and in the hydraulic conductivity curve were observed as a result of the presence of century-old charcoal. For this soil, the charcoal particles may have predominantly replaced organo-mineral micromass with similar pore size characteristics, with no resulting effect on the water characteristic curves of the soil.

5 | CONCLUSION

For the first time, chemical as well as physical properties were measured along transects of century-old charcoal content in kiln sites on three soils characterized by different texture (silt loam, loam and sandy loam) in Wallonia.

For all three sites, the presence of historical charcoal increased significantly the soil cation exchange capacity and bivalent cation contents. Although both

soil particle densities and bulk densities decreased with increasing charcoal-C content, total porosity was unaffected. Consequently, the charcoal does not appear to have a structuring effect (in the sense of increased porosity) but rather an effect on the pore size distribution at constant total porosity. Although some significant effects of charcoal on the soil hydrodynamic properties were observed (e.g., water retention in the mesopore range for the sandy loam; hydraulic conductivity at pF values between 1.5 and 2 for the silt loam), the present study highlights a limited effect of century-old charcoal across the range of soils investigated here. Measurements of soil physical properties at short (a few years) and intermediate time scales (10–20 years after burying biochar in soil) would be very interesting to test whether this reflects a long-term decreasing trend in biochar effectiveness. On the other hand, analysis of the pore size distribution of century-old charcoal with mercury porosimetry or X-ray tomography as well as soil observation by means of optical or electron microscopy may help clarify the role played by charcoal in soil structure. Further research may also be needed to confirm the observed trends over a wider range of soil types.

ACKNOWLEDGEMENTS

We thank J. Lefour and S. François from the Earth and Life Institute of the Université Catholique de Louvain for their help during the measurement of the water retention and hydraulic conductivity curves. We are grateful to B. Hardy from the CRA-W, V. Burgeon from the Université of Liège and T. Kervyn from the SPW for their help with different parts of this research. We thank the farmers who made their fields available.

AUTHOR CONTRIBUTIONS

Martin Zanutel: Conceptualization; data curation; formal analysis; funding acquisition; investigation; methodology; resources; software; validation; visualization; writing; original draft; writing; review and editing. **Sarah Garré:** Conceptualization; formal analysis; methodology; supervision; validation. **Charles Bielders:** Conceptualization; formal analysis; funding acquisition; methodology; supervision; validation.

DATA AVAILABILITY STATEMENT

Data available on request from the authors The data that support the findings of this study are available from the corresponding author upon reasonable request.

ORCID

Martin Zanutel https://orcid.org/0000-0002-6924-0649
Sarah Garré https://orcid.org/0000-0001-9025-5282
Charles L. Bielders https://orcid.org/0000-0003-2865-4236

REFERENCES

Abel, S., Peters, A., Trinks, S., Schonsky, H., Facklam, M., & Wessolek, G. (2013). Impact of biochar and hydrochar addition on water retention and water repellency of sandy soil. *Geoderma*, *202-203*, 183–191. https://doi.org/10.1016/j.geoderma.2013.03.003

Biederman, L. A., & Harpole, W. S. (2013). Biochar and its effects on plant productivity and nutrient cycling: A meta-analysis. *GCB Bioenergy*, *5*, 202–214. https://doi.org/10.1111/gcbb.12037

Bielders, C. L., De Backer, L. W., & Delvaux, B. (1990). Particle density of volcanic soils as measured with a gas pycnometer. *Soil Science Society of America Journal*, *54*(3), 822–826. https://doi.org/10.2136/sssaj1990.03615995005400030034x

Blake, G. R., & Hartge, K. (1986). Bulk density. In A. Klute (Ed.), *Methods of soil analysis: Part 1 physical and mineralogical methods* (pp. 363–375). Madison, WI: American Society of Agronomy. https://doi.org/10.2136/sssabookser5.1.2ed.c13

Blanco-Canqui, H. (2017). Biochar and soil physical properties. *Soil Science Society of America Journal*, *81*, 687–711. https://doi.org/10.2136/sssaj2017.01.0017

Brewer, C. E., Chuang, V. J., Masiello, C. A., Gonnermann, H., Gao, X., Dugan, B., … Daviese, C. (2014). New approaches to measuring biochar density and porosity. *Biomass and Bioenergy*, *66*, 176–185. https://doi.org/10.1016/j.biombioe.2014.03.059

Brodowski, S., John, B., Flessa, H., & Amelung, W. (2006). Aggregate-occluded black carbon in soil. *European Journal of Soil Science*, *57*, 539–546. https://doi.org/10.1111/j.1365-2389.2006.00807.x

Bronick, C. J., & Lal, R. (2005). Soil structure and management: A review. *Geoderma*, *124*, 3–22. https://doi.org/10.1016/j.geoderma.2004.03.005

Burgeon, V., Fouché, J., Leifeld, J., Chenu, C., & Cornelis, J.-T. (2021). Organo-mineral associations largely contribute to the stabilization of century-old pyrogenic organic matter in cropland soils. *Geoderma*, *388*, 114841. https://doi.org/10.1016/j.geoderma.2020.114841

Cassel, D. K., & Nielsen, D. R. (1986). Field capacity and available water capacity. In A. Klute (Ed.), *Methods of soil analysis: Part 1 physical and mineralogical methods* (pp. 901–926). Madison, WI: American Society of Agronomy. https://doi.org/10.2136/sssabookser5.1.2ed.c36

Cheng, C.-H., Lehmann, J., Thies, J. E., Burton, S. D., & Engelhard, M. H. (2006). Oxidation of black carbon by biotic and abiotic processes. *Organic Geochemistry*, *37*, 1477–1488. https://doi.org/10.1016/j.orggeochem.2006.06.022

Cheng, C.-H., Lehmann, J., & Engelhard, M. H. (2008). Natural oxidation of black carbon in soils: Changes in molecular form and surface charge along a climosequence. *Geochimica et Cosmochimica Acta*, *72*, 1598–1610. https://doi.org/10.1016/j.gca.2008.01.010

Criscuoli, I., Alberti, G., Baronti, S., Favilli, F., Martinez, C., Calzolari, C., … Miglietta, F. (2014). Carbon sequestration and fertility after centennial time scale incorporation of charcoal into soil. *PLoS One*, *9*, 1–11. https://doi.org/10.1371/journal.pone.0091114

Danielson, R. E., & Sutherland, P. L. (1986). Porosity. In A. Klute (Ed.), *Methods of soil analysis: Part 1 physical and mineralogical*

methods (pp. 443–461). Madison, WI: American Society of Agronomy. https://doi.org/10.2136/sssabookser5.1.2ed.c18

Ding, Y., Liu, Y., Liu, S., Li, Z., Tan, X., Huang, X., … Zheng, B. (2016). Biochar to improve soil fertility. A review. *Agronomy for Sustainable Development*, *36*(2), 1–18. https://doi.org/10.1007/s13593-016-0372-z

Du, Z.-L., Zhao, J.-K., Wang, Y.-D., & Zhang, Q.-Z. (2017). Biochar addition drives soil aggregation and carbon sequestration in aggregate fractions from an intensive agricultural system. *Journal of Soils and Sediments*, *17*(3), 581–589. https://doi.org/10.1007/s11368-015-1349-2

Durner, W. (1994). Hydraulic conductivity estimation for soils with heterogeneous pore structure. *Water Resources Research*, *32*(9), 211–223. https://doi.org/10.1029/93WR02676

Edeh, I. G., Mašek, O., & Buss, W. (2020). A meta-analysis on biochar's effects on soil water properties – New insights and future research challenges. *Science of the Total Environment*, *714*, 136857. https://doi.org/10.1016/j.scitotenv.2020.136857

Faghih, F., Emadi, M., Sadegh-Zadeh, F., & Bahmanyar, M. A. (2018). Long-term charcoal-induced changes to soil properties in temperate regions of northern Iran. *Journal of Forestry Research*, *30*, 1063–1071. https://doi.org/10.1007/s11676-018-0641-6

Hardie, M., Clothier, B., Bound, S., Oliver, G., & Close, D. (2014). Does biochar influence soil physical properties and soil water availability? *Plant and Soil*, *376*, 347–361. https://doi.org/10.1007/s11104-013-1980-x

Hardy, B., & Dufey, J. (2012). Estimation des besoins en charbon de bois et en superficie forestierepour la siderurgie wallonne pre-industrielle (1750–1830) deuxième partie: les besoins en superficie forestiere. *Revue Forestière Française*, *6*, 799–806.

Hardy, B., Cornelis, J.-T., Houben, D., Lambert, R., & Dufey, J. E. (2016). The effect of pre-industrial charcoal kilns on chemical properties of forest soil of Wallonia, Belgium. *European Journal of Soil Science*, *67*, 206–216. https://doi.org/10.1111/ejss.12324

Hardy, B., Cornelis, J.-T., Houben, D., Leifeld, J., Lambert, R., & Dufey, J. E. (2016). Evaluation of the long-term effect of biochar on properties of temperate agricultural soil at pre-industrial charcoal kiln sites in Wallonia, Belgium. *European Journal of Soil Science*, *68*(1), 80–89. https://doi.org/10.1111/ejss.1239

Hardy, B., Leifeld, J., Knicker, H., Dufey, J. E., Deforce, K., & Cornelis, J.-T. (2017). Long term change in chemical properties of preindustrial charcoal particles aged in forest and agricultural temperate soil. *Organic Geochemistry*, *107*, 33–45. https://doi.org/10.1016/j.orggeochem.2017.02.008

Hernandez-Soriano, M. C., Kerré, B., Goos, P., Hardy, B., Dufey, J., & Smolders, E. (2016). Long-term effect of biochar on the stabilization of recent carbon: Soils with historical inputs of charcoal. *GCB Bioenergy*, *8*, 371–381. https://doi.org/10.1111/gcbb.12250

Hyväluoma, J., Kuljun, S., Hannula, M., Wikberg, H., Källi, A., & Rasa, K. (2018). Quantitative characterization of pore structure of several biochars with 3D imaging. *Environmental Science and Pollution Research*, *25*(26), 1–11. https://doi.org/10.1007/s11356-017-8823-x

Jeffery, S., Verheijen, F. G. A., van der Velde, M., & Bastos, A. C. (2011). A quantitative review of the effects of biochar application to soils on crop productivity using meta-analysis. *Agriculture, Ecosystems & Environment*, *144*, 175–187. https://doi.org/10.1016/j.agee.2011.08.015

Jien, S.-H., & Wang, C.-S. (2013). Effects of biochar on soil properties and erosion potential in a highly weathered soil. *Catena*, *110*, 225–233. https://doi.org/10.1016/j.catena.2013.06.021

Jien, S.-H., Wang, C.-C., Lee, C.-H., & Lee, T.-Y. (2015). Stabilization of organic matter by biochar application in compost-amended soils with contrasting pH values and textures. *Sustainability*, *7*(10), 13317–13333. https://doi.org/10.3390/su71013317

Kerré, B., Bravo, C. T., Leifeld, J., Cornelissen, G., & Smolders, E. (2016). Historical soil amendment with charcoal increases sequestration of non-charcoal carbon: A comparison among methods of black carbon quantification. *European Journal of Soil Science*, *67*, 324–331. https://doi.org/10.1111/ejss.12338

Kerré, B., Willaert, B., Cornelis, Y., & Smolders, E. (2017). Long-term presence of charcoal increases maize yield in Belgium due to increased soil water availability. *European Journal of Agronomy*, *91*, 10–15. https://doi.org/10.1016/j.eja.2017.09.003

Kerré, B., Willaert, B., & Smolders, E. (2017). Lower residue decomposition in historically charcoal-enriched soils is related to increased adsorption of organic matter. *Soil Biology & Biochemistry*, *104*, 1–7. https://doi.org/10.1016/j.soilbio.2016.10.007

Knicker, H. (2011). Pyrogenic organic matter in soil: Its origin and occurrence, its chemistry and survival in soil environments. *Quaternary International*, *243*, 251–263. https://doi.org/10.1016/j.quaint.2011.02.037

Lakanen, E., & Erviö, R. (1971). A comparison of eight extractants for the determination of plant available micronutrients in soils. *Acta Agralia Fennica*, *123*, 223–232.

Lehmann, J., Liang, B., Solomon, D., Lerotic, M., Luizão, F., Kinyangi, J., … Jacobsen, C. (2005). Near-edge X-ray absorption fine structure (NEXAFS) spectroscopy for mapping nano-scale distribution of organic carbon forms in soil: Application to black carbon particles. *Global Biogeochemical Cycles*, *19*, GB1013. https://doi.org/10.1029/2004GB002435

Lehmann, J., Gaunt, J., & Rondon, M. (2006). Bio-char sequestration in terrestrial ecosystems – A review. *Mitigation and Adaptation Strategies for Global Change*, *11*, 395–419. https://doi.org/10.1007/s11027-005-9006-5

Lehmann, J. (2007). A handful of carbon. *Nature*, *447*, 10–11. https://doi.org/10.1038/447143a

Lehmann, J., & Joseph, S. (2009). *Biochar for environmental management: Science and technology*. London: Earthscan.

Lehmann, J., & Joseph, S. (2015). Biochar for environmental management: An introduction. In J. Lehmann & S. Joseph (Eds.), *Biochar for environmental management* (pp. 1–14). London, England: Science, Technology and Implementation. https://doi.org/10.4324/9780203762264

METER Group. (2018). WP4C: Dew Point PotentiaMeter (Operator's Manual).

Omondi, M. O., Xia, X., Nahayo, A., Liu, X., Korai, P. K., & Pan, G. (2016). Quantification of biochar effects on soil hydrological properties using meta-analysis of literature data. *Geoderma*, *274*, 28–34. https://doi.org/10.1016/j.geoderma.2016.03.029

Pertassek, T., Peters, A., & Durner, W. (2015). *HYPROP-FIT software User's manual, V.3.0. METER group AG, Mettlacher Str. 8, 81379* (p. 66). München, Germany. UMS GmbH.

Peters, A., & Durner, W. (2008). Simplified evaporation method for determining soil hydraulic properties. *Journal of Hydrology*, *356*, 147–162. https://doi.org/10.1016/j.jhydrol.2008.04.016

Pituello, C., Dal Ferro, N., Francioso, O., Simonetti, G., Berti, A., Piccoli, I., ... Morari, F. (2018). Effects of biochar on the dynamics of aggregate stability in clay and sandy loam soils. *European Journal of Soil Science*, *69*, 827–842. https://doi.org/10.1111/ejss.12676

Plötze, M., & Niemz, P. (2011). Porosity and pore size distribution of different wood types as determined by mercury intrusion porosimetry. *European Journal of Wood and Wood Products*, *69*, 649–657. https://doi.org/10.1007/s00107-010-0504-0

Rabot, E., Wiesmeier, M., Schlüter, S., & Vogel, H.-J. (2018). Soil structure as an indicator of soil functions: A review. *Geoderma*, *314*, 122–137. https://doi.org/10.1016/j.geoderma.2017.11.009

Razzaghi, F., Obour, P. B., & Arthur, E. (2020). Does biochar improve soil water retention? A systematic review and meta-analysis. *Geoderma*, *361*, 114055. https://doi.org/10.1016/j.geoderma.2019.114055

Richards, L. A., & Fireman, M. (1943). Pressure plate apparatus for measuring moisture sorption and transmission by soils. *Soil Science*, *56*(6), 395–404. https://doi.org/10.1097/00010694-194312000-00001

Schindler, U., von Unold, G., Durner, W., & Müller, L. (2010). Evaporation method for measuring unsaturated hydraulic properties of soils: Extending the range. *Soil Science Society of American Journal*, *74*, 1071–1083. https://doi.org/10.2136/sssaj2008.0358

Schneider, A., Hirscha, F., Bonhagea, A., Raab, A., & Raab, T. (2020). The soil moisture regime of charcoal-enriched land use legacy sites. *Geoderma*, *336*, 114241. https://doi.org/10.1016/j.geoderma.2020.114241

Şeker, C., & Manirakiza, N. (2020). Effectiveness of compost and biochar in improving water retention characteristics and aggregation of a sandy clay cloam soil under wind erosion. *Carpathian Journal of Earth and Environmental Sciences*, *15*(1), 5–18. https://doi.org/10.26471/cjees/2020/015/103

Singh, N., Abiven, S., Torn, M. S., & Schmidt, M. W. I. (2012). Fire-derived organic carbon in soil turns over on a centennial scale. *Biogeosciences*, *9*, 2847–2857. https://doi.org/10.5194/bg-9-2847-2012

Solomon, D., Lehmann, J., Thies, J., Schäfer, T., Liang, B., Kinyangi, J., ... Skjemstad, J. (2007). Molecular signature and sources of biochemical recalcitrance of organic C in Amazonian dark earths. *Geochimica et Cosmochimica Acta*, *71*, 2285–2298. https://doi.org/10.1016/j.gca.2007.02.014

Trupiano, D., Cocozza, C., Baronti, S., Amendola, C., Vaccari, F. P., Lustrato, G., ... Scippa, G. S. (2017). The effects of biochar and its combination with compost on lettuce (*Lactuca sativa* L.) growth, soil properties, and soil microbial activity and abundance. *International Journal of Agronomy*, *2017*, 1–12. https://doi.org/10.1155/2017/3158207

Van Genuchten, M. T. (1980). A closed-form equation for predicting the hydraulic conductivity of unsaturated soils. *Soil Science Society of American Journal*, *44*(5), 892–898. https://doi.org/10.2136/sssaj1980.03615995004400050002x

Veron, P., Bah, B., Bracke, C., Lejeune, P., Rondeux, J., Bock, L. & Mokadem, A.I. (2005). The digital soil map of Wallonia (DSMW/CNSW). In: Proceedings of XXII International Cartographic Conference at A Coruna, Spain, July 11–16, 2005, 8pp. Spain: The International Cartographic Association.

Wildman, J., & Derbyshire, F. (1991). Origins and functions of macroporosity in activated carbons from coal and wood precursors. *Fuel*, *70*(5), 655–661.

Yi, S., Chang, Y. C., & Imhoff, P. T. (2020). Predicting water retention of biochar-amended soil from independent measurements of biochar and soil properties. *Advances in Water Resources*, *142*, 103638. https://doi.org/10.1016/j.advwatres.2020.103638

How to cite this article: Zanutel, M., Garré, S., & Bielders, C. L. (2021). Long-term effect of biochar on physical properties of agricultural soils with different textures at pre-industrial charcoal kiln sites in Wallonia (Belgium). *European Journal of Soil Science*, 1–17. https://doi.org/10.1111/ejss.13157